Available online at www.sciencedirect.com
SCIENCE DIRECT®
Journal of Solid State Chemistry 177 (2004) 3839–3842
JOURNAL OF SOLID STATE CHEMISTRY
www.elsevier.com/locate/jssc

Rapid Communication

First electrochemical growth of $Tb_{16}O_{30}$ single crystal

Nobuhito Imanaka*, Toshiyuki Masui, Young Woon Kim

Department of Applied Chemistry, Faculty of Engineering, Handai Frontier Research Center, Osaka University, 2-1 Yamadaoka, Suita, Osaka 565-0871, Japan

Received 1 June 2004; received in revised form 9 July 2004; accepted 12 July 2004
Available online 27 August 2004

Abstract

Single crystals of $Tb_{16}O_{30}$ ($TbO_{1.875}$) were successfully grown for the first time by DC electrolysis of the Tb^{3+} ion conducting $Tb_2(MoO_4)_3$ solid electrolyte at 11 V, 900 °C. The $Tb_{16}O_{30}$ phase is the intermediate phase of fluorite-related rare earth oxides and it is extremely difficult to grow in a single crystal form, because this intermediate phase is usually obtained as one of the mixture of the fluorite related TbO_x phases. Because there are many non-stoichiometric phases in the terbium oxide system, it is impossible to grow a specific intermediate phase in a single crystal form by the conventional methods via melt. Although single crystals of TbO_x have been recently obtained by anodic electrocrystallization from alkaline hydroxide melts containing $TbCl_3$, the composition has been confirmed to be TbO_x with $1.75 < x < 1.82$. On the contrary, the presently developed DC electrolysis method can be simply applicable at moderate temperatures around 900 °C to artificially grow an intermediate phase of $Tb_{16}O_{30}$ ($x = 1.875$) in a single crystal form, which was evidenced by the electron diffraction patterns for each particle.

PACS: 81.10.Jt; 61.14.Lj; 83.70.Bi; 72.80.−r

Keywords: $Tb_{16}O_{30}$; Solid electrolytes; Crystal growth; Electrolysis

1. Introduction

Cerium, praseodymium, and terbium oxides have an extensive and complex homologous series of oxygen-deficient, fluorite-related phases, R_nO_{2n-2m}, with varying oxygen/vacancy and R^{III}/R^{IV} ratios [1,2]. These are intermediate mixed-valent compounds with compositions between R_2O_3 and RO_2. Among them, seven structures of Ce_7O_{12} [3], Pr_7O_{12} [4], Pr_9O_{16} [5], $Pr_{10}O_{18}$ ($Pr_{40}O_{72}$) [6], $Pr_{12}O_{22}$ ($Pr_{24}O_{44}$) [7], Tb_7O_{12} and $Tb_{11}O_{20}$ [8] have been determined using neutron powder diffraction data. All other members of the series have been identified in the high-resolution transmission electron microscopic observation. However, there are a few reports on the structure of the intermediate terbium oxide especially for bulky samples.

The non-stoichiometric fluorite-related terbium oxide is usually prepared by annealing Tb_2O_3 (sesquioxide) or Tb_4O_7 (average composition of a stable mixed-valence oxide composed of mixtures) maintaining a defined oxygen pressure [8–10]. Only two references have been reported on the synthesis of larger single crystals [11,12]. Single crystals of the oxygen deficient TbO_x with $1.75 < x < 1.82$ have been recently grown by anodic electrocrystallization from alkaline hydroxide melts containing $TbCl_3$ [11], and single crystals of intermediate terbium oxide of $Tb_{11}O_{20}$ ($TbO_{1.818}$) were grown by the hydrothermal method [12]. However, there is no report on the single crystal growth of non-stoichiometric TbO_x with $1.82 < x$.

In our previous study, we have elucidated that Sc_2O_3 [13,14] and aluminum oxide [15] single crystal was successfully grown by a simple DC electrolysis method at temperatures below 1000 °C. The selective growth of these crystals has been achieved by electrolyzing the

*Corresponding author. Fax: +81-6-6879-7354.
E-mail address: imanaka@chem.eng.osaka-u.ac.jp (N. Imanaka).

0022-4596/$ - see front matter © 2004 Elsevier Inc. All rights reserved.
doi:10.1016/j.jssc.2004.07.015

Sc^{3+} or Al^{3+} ion conducting solid electrolyte of $M_2(MoO_4)_3$ (M = Sc or Al). In this process, the successive DC electrolysis supplies scandium or aluminum metal from inside the solid electrolyte produced by the reduction of their ions migrated forward the cathodic surface and finally the stable C-type cubic Sc_2O_3 or δ-type tetragonal Al_2O_3 single crystals are grown in air atmosphere at moderate temperatures. Here, it is notable that intermediate δ-phase was grown in a single crystal form in the case of Al_2O_3 growth.

In this communication, therefore, intermediate terbium oxide $Tb_{16}O_{30}$ ($TbO_{1.875}$) was electrochemically grown in a single crystal form at moderate temperature as low as 900 °C by using $Tb_2(MoO_4)_3$ as the Tb^{3+}-conductiong solid electrolyte [16,17]. The Tb^{3+} cations accept electrons and are reduced to terbium metal in atomic scale when they reached to the cathodic surface. The terbium metal is oxidized immediately in the high temperature atmospheric air (900 °C), growing by the supply of Tb metal from inside the $Tb_2(MoO_4)_3$ solid electrolyte at the same time. Therefore, the higher terbium oxides, TbO_x ($x > 1.82$, e.g., $Tb_{16}O_{30}$), are expected to be grown in a single crystal form without difficulty.

2. Experimental

A stoichiometric amount of Tb_4O_7 (purity 99.9%) and MoO_3 (purity 99.9%) was ground and mixed in a mortar. The mixture was calcined at 750 °C for 12 h in a flow of dry air to prepare $Tb_2(MoO_4)_3$. The resulting powder was made into pellets (10 mm in diameter and 0.8 mm in thickness) and sintered at 1000 °C for 12 h in a flow of dry air. The sample pellet sintered was placed between two ion-blocking Pt electrodes for the crystal growth electrolysis as illustrated in Fig. 1. The electrolysis was carried out by DC voltage of 11 V at 900 °C for 2 weeks in air.

The particles grown were characterized with a scanning electron microscope (SEM, Hitachi S-4300SD). The sample was sputter-coated with a gold layer before SEM observation to minimize any possible surface charging effects. The particle size distribution and the average particle size were determined by measuring the mean length of the shortest and the longest diameters in a particle for more than 200 particles on the SEM photograph. Selected area electron diffraction (SAED) measurement was performed with a transmission electron microscope (TEM, Hitachi, H-800) equipped with a tilting device and operating at 200 kV. The prepared particles were rinsed out from the matrix with ethanol and then supported on an amorphous carbon film mounted on a copper grid. Images were recorded under axial illumination at an approximate Scherzer focus, with a point resolution better than 0.194 nm. The diameter of the objective aperture was 20 μm, which was large enough to include some low-indexed diffraction spots from the sample.

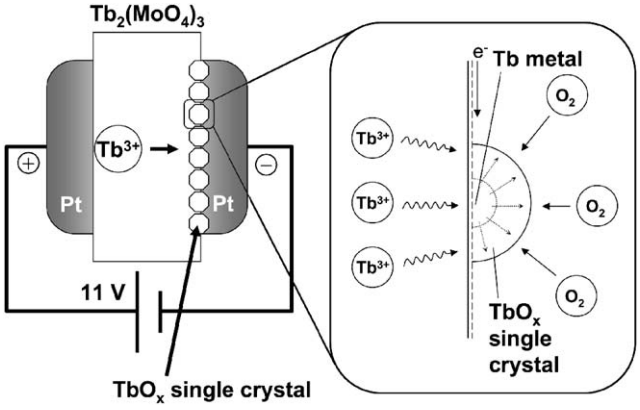

Fig. 1. Schematic illustration of TbO_x single crystal growth method by DC electrolysis.

3. Results and discussion

Fig. 2 shows the X-ray powder diffraction patterns of the sample obtained on the cathodic surface of the $Tb_2(MoO_4)_3$ solid electrolyte after the electrolysis for 2

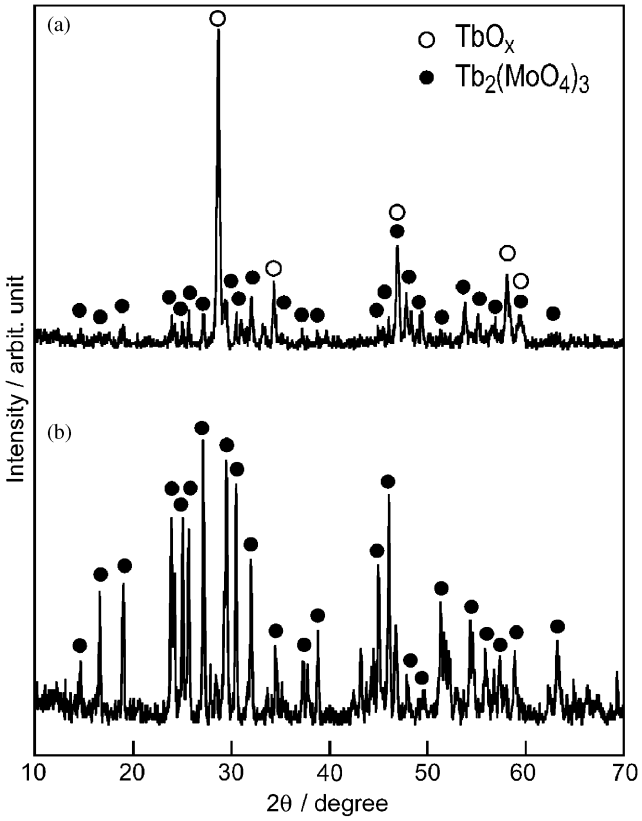

Fig. 2. X-ray powder diffraction results for the crystal samples: patterns for the cathodic surface of the electrolyzed $Tb_2(MoO_4)_3$ solid electrolyte for 2 weeks (a) and $Tb_2(MoO_4)_3$ pellet before electrolysis (b).

weeks and the $Tb_2(MoO_4)_3$ before electrolysis. The XRD patterns obtained after the electrolysis were identical to those of fluorite TbO_x, which was featured by the broadened lines of fluorite pattern [18]. No impurity peaks other than TbO_x and $Tb_2(MoO_4)_3$ were observed.

Fig. 3 depicts the SEM image of the prepared particles obtained by the electrolysis of $Tb_2(MoO_4)_3$ at 900 °C and 11 V for 2 weeks. The cathodic surface was covered with well-defined polyhedral particles, while no deposits were recognized on the anodic surface. The particle formation was not observed on another pellet of $Tb_2(MoO_4)_3$ polycrystals subjected to the same experimental conditions without the electrolysis. Well-defined polyhedral tabular particles ranging from 0.1 to 1.2 μm were obtained by the electrolysis. The particle size distribution histogram of the particles shown in Fig. 4 was obtained from the calculation of the diameter for more than 200 particles on the SEM photograph. The average particle size was 0.42 μm, and the standard deviation was estimated to be 0.19 μm.

In order to identify whether each particle is exactly a single crystal form or not, SAED pattern measurements were carried out. The SAED pattern was obtained for a particle on a TEM copper grid, and energy dispersive X-ray analyzer equipped with the TEM device showed no impurities in the particle. The sharp diffraction spots in Fig. 5 clearly indicate the superior crystallinity of the particle. The net pattern was recorded along a $\langle 110 \rangle_F$ direction (where F stands for fluorite) and consistently corresponded to that of [041] zone axis pattern of the π-phase ($Tb_{16}O_{30}$) [19] which is the most highly oxidized and ordered intermediate phase in the R_nO_{2n-2m} series of fluorite related phases in any binary rare earth oxides [10]. The diffraction spots obtained above explicitly elucidate that the $Tb_{16}O_{30}$ particle exists as a single crystal form on the surface of $Tb_2(MoO_4)_3$ polycrystalline matrices. The superstructure determined from the electron diffraction pattern was assigned to a monoclinic lattice with $a = 12.6$ Å, $b = 29.7$ Å, $c = 14.8$ Å, and $\beta = 125°$ within the error of $\pm 0.5\%$.

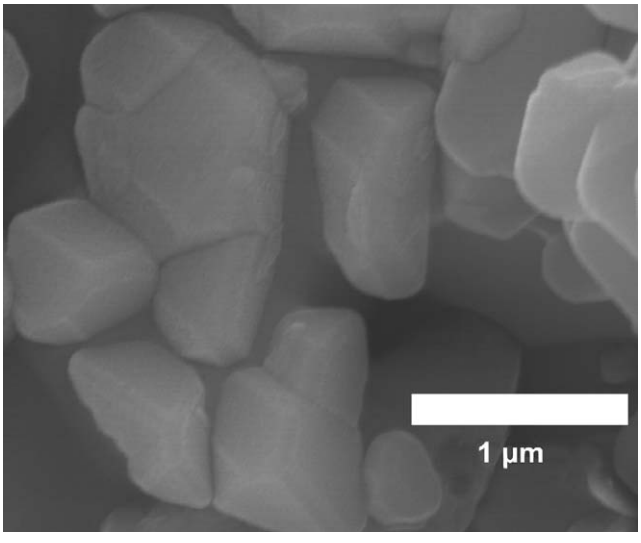

Fig. 3. SEM photograph of the cathodic surface of the $Tb_2(MoO_4)_3$ pellet after electrolyzing at 900 °C for 2 weeks at 11 V.

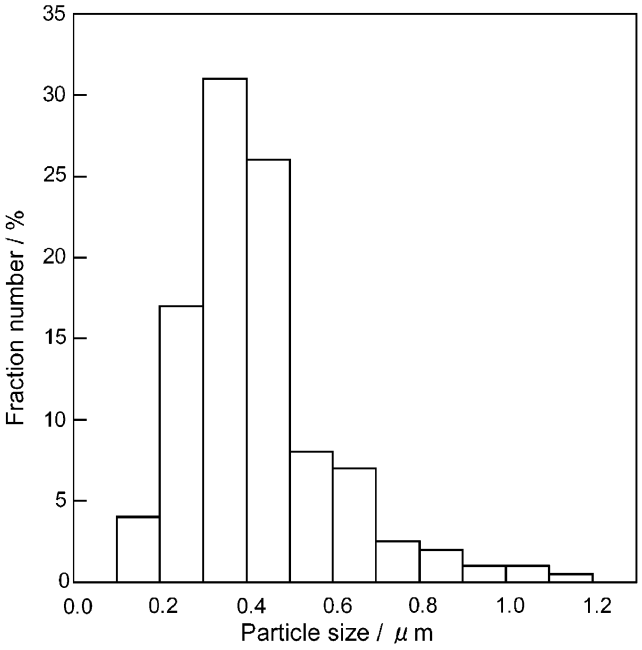

Fig. 4. Particle size distribution histogram of the TbO_x particles.

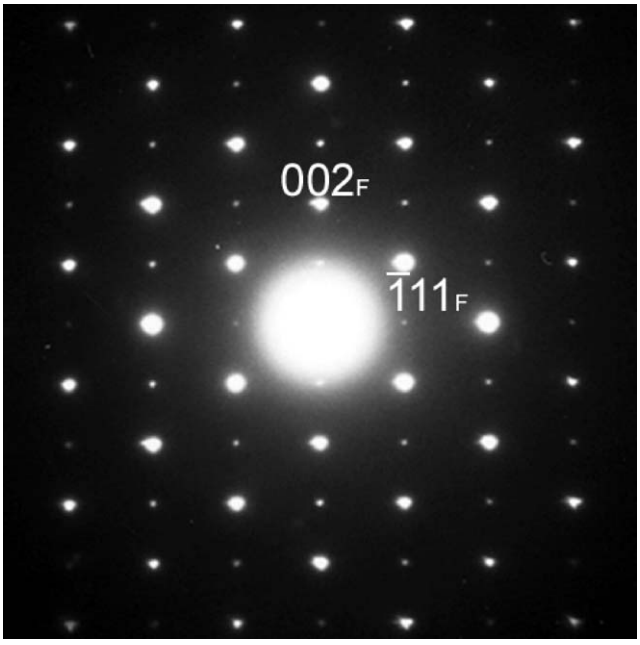

Fig. 5. Electron diffraction pattern of the TbO_x particle along a $\langle 110 \rangle_F$ direction. It corresponds to that of $[041]_\pi$ superlattice spots ($Tb_{16}O_{30}$).

The mechanism of the single crystal growth can be explained as follows. The DC voltage applied (11 V) during the electrolysis was much higher than the decomposition voltage of $Tb_2(MoO_4)_3$ (ca. 0.5 V) determined by measuring the *I–V* characteristics of the $Tb_2(MoO_4)_3$ solid electrolyte. A considerable higher DC voltage as compared with the decomposition voltage of $Tb_2(MoO_4)_3$ facilitates the $Tb_2(MoO_4)_3$ decomposition to Tb^{3+} ions at the anode and the MoO_3 and gaseous O_2 formation at the anode according to the following half-cell reaction:

$$2[MoO_4]^{2-} \rightarrow 2MoO_3 + O_2 + 4e^-.$$

Since MoO_3 produced at the anode readily sublimates during the electrolysis because the electrolysis was conducted at 900 °C, which is above the MoO_3 sublimation temperature of around 750–800 °C, Tb^{3+} ions are successively produced at the anodic surface and conduct through the $Tb_2(MoO_4)_3$ bulk by ionic conduction from the anode to the Pt cathode direction during the electrolysis. When the Tb^{3+} ions reach at the cathode, they are reduced to the metal state at the interface between the sample and the cathode.

$$Tb^{3+} + 3e^- \rightarrow Tb.$$

The Tb metal is immediately oxidized to $Tb_{16}O_{30}$ from the surface of the Tb deposits due to electrolyzing in air (see Fig. 1).

$$16Tb + 15O_2 \rightarrow Tb_{16}O_{30}.$$

Because the Tb^{3+} ions are steadily and gradually supplied from inside the $Tb_2(MoO_4)_3$ electrolyte by the electrolysis, Tb metal is successively supplied overall cathodic surface equally. As a result, terbium oxide single crystals in similar size are grown on the cathodic surface of the $Tb_2(MoO_4)_3$ solid electrolyte. In addition, the subsequent oxidation of the Tb metal is carried out under the moderate heating condition. Therefore, the homogeneous $Tb_{16}O_{30}$ π-phase was produced in a single crystal form in spite that this phase was believed to be metastable and the existence of the π-phase has been only confirmed [10]. The single crystal growth of the π-$Tb_{16}O_{30}$ phase has been realized for the first time by the present study.

In conclusion, single crystals of intermediate $Tb_{16}O_{30}$ form were successfully grown for the first time by a simple DC electrolysis method at the moderate temperature of 900 °C. This method will be applicable to grow intermediate phase of the fluorite-related other rare earth oxides in a single crystal form, from the lower to higher oxidation state by adjusting oxygen partial pressure or growth temperature, even if the phase is metastable.

Acknowledgments

The authors sincerely thank Dr. Ken-ichi Nakayama and Prof. Dr. Masaaki Yokoyama (Osaka University) for their assistance with the SEM observation. We are also grateful to Dr. Takao Sakata and Prof. Dr. Hirotaro Mori (Osaka University) for their assistance with the SAED measurement. The present work was partially supported by a Grant-in-Aid for Scientific Research No. 15550172 from The Ministry of Education, Science, Sports and Culture. This work was also partially supported by the Industrial Technology Research Grant Program in '02 (project ID: 02A27004c) from the New Energy and Industrial Technology Development Organization (NEDO) based on funds provided by the Ministry of Economy, Trade and Industry, Japan (METI).

References

[1] Z.C. Kang, L. Eyring, Aust. J. Chem. 49 (1997) 981–996.
[2] Z.C. Kang, L. Eyring, J. Alloys Compds. 249 (1997) 206–212.
[3] S.P. Ray, D.E. Cox, J. Solid State Chem. 15 (1975) 333–343.
[4] R.B. Von Dreele, L. Eyring, Acta Crystallogr. B 31 (1975) 971–974.
[5] J. Zhang, R.B. Von Dreele, L. Eyring, J. Solid State Chem. 118 (1995) 133–140.
[6] J. Zhang, R.B. Von Dreele, L. Eyring, J. Solid State Chem. 118 (1995) 141–147.
[7] J. Zhang, R.B. Von Dreele, L. Eyring, J. Solid State Chem. 122 (1996) 53–58.
[8] J. Zhang, R.B. Von Dreele, L. Eyring, J. Solid State Chem. 104 (1993) 21–32.
[9] P. Kunzmann, L. Eyring, J. Solid State Chem. 14 (1975) 229–237.
[10] R.T. Tuenge, L. Eyring, J. Solid State Chem. 41 (1982) 75–89.
[11] M. Malchus, M. Jansen, Solid State Sciences 2 (2000) 65–70.
[12] M. Mckelvy, L. Eyring, J. Cryst. Growth 62 (1983) 635–638.
[13] N. Imanaka, Y.W. Kim, T. Masui, G. Adachi, Cryst. Growth Des. 3 (2003) 289–290.
[14] T. Masui, Y.W. Kim, N. Imanaka, G. Adachi, J. Alloys Compds. 374 (2004) 97–100.
[15] N. Imanaka, T. Masui, Y.W. Kim, Cryst. Growth Des. 4 (2004) 663–665.
[16] N. Imanaka, T. Ueda, Y. Okazaki, S. Tamura, G. Adachi, Chem. Mater. 12 (2000) 1910–1913.
[17] N. Imanaka, Y. Kobayashi, S. Tamura, G. Adachi, Solid State Ionics 136–137 (2000) 319–324.
[18] Z.C. Kang, L. Eyring, J. Solid State Chem. 75 (1988) 60–72.
[19] C. López-Cartes, J.A. Pérez-Omil, J.M. Pintado, J.J. Calvino, Z.C. Kang, L. Eyring, Ultramicroscopy 80 (1999) 19–39.